### Title
Inhibition of stress fiber formation preserves blood–brain barrier after intracerebral hemorrhage in mice




### Journal
Cerebrovascular and Brain Metabolism Reviews, 38(1)

### ISSN
1040-8827



### Authors
Manaenko, Anatol
Yang, Peng
Nowrangi, Derek
et al.



### Publication Date
2018

### DOI
10.1177/0271678x16679169

Peer reviewed

*Original Article*

JCBFM

Journal of Cerebral Blood Flow & Metabolism
2018, Vol. 38(1) 87–102

DOI: 10.1177/0271678X16679169
journals.sagepub.com/home/jcbfm
SAGE

# Inhibition of stress fiber formation preserves blood–brain barrier after intracerebral hemorrhage in mice

**Anatol Manaenko[1,2,*], Peng Yang[1,3,*], Derek Nowrangi[1], Enkhjargal Budbazar[1], Richard E Hartman[4], Andre Obenaus[5], William J Pearce[1], John H Zhang[1,6,7] and Jiping Tang[1]**

## Abstract

Intracerebral hemorrhage (ICH) represents the deadliest subtype of all strokes. The development of brain edema, a consequence of blood–brain barrier (BBB) disruption, is the most life-threatening event after ICH. Pathophysiological conditions activate the endothelium, one of the components of BBB, inducing rearrangement of the actin cytoskeleton. Upon activation, globular actin assembles into a filamentous actin resulting in the formation of contractile actin bundles, stress fibers. The contraction of stress fibers leads to the formation of intercellular gaps between endothelial cells increasing the permeability of BBB. In the present study, we investigated the effect of ICH on stress fiber formation in CD1 mice. We hypothesized that ICH-induced formation of stress fiber is triggered by the activation of PDGFR-β and mediated by the cortactin/RhoA/LIMK pathway. We demonstrated that ICH induces formation of stress fibers. Furthermore, we demonstrated that the inhibition of PDGFR-β and its downstream reduced the number of stress fibers, preserving BBB and resulting in the amelioration of brain edema and improvement of neurological functions in mice after ICH.

## Keywords

Cortactin, intracerebral hemorrhage, LIM kinase, PDGFR-β, stress fibers

Received 22 April 2016; Revised 21 September 2016; Accepted 14 October 2016

## Introduction

Intracerebral hemorrhage (ICH) represents the deadliest subtype of all strokes. Brain edema, a life-threatening consequence of ICH, significantly contributes to a high mortality after ICH. The most common type of brain edema, vasogenic edema, results from increased blood–brain barrier (BBB) permeability.[1–4] The BBB permeability is regulated by adherens and tight junctions. While the function of adherens junctions is to hold neighboring primary epithelial cells together, the tight junctions mediate the gate functions of the BBB and prevent solutes from paracellular diffusion.[5] Under pathophysiological conditions, the endothelium, one of the components of BBB, is activated, inducing rearrangement of the actin cytoskeleton. Actin in resting endothelium is present as a monomeric globular actin (G-actin). Upon activation, G-actin assembles into a filamentous actin (F-actin) and the shift from G-actin to F-actin results in the formation of contractile actin

[1]Department of Physiology and Pharmacology, Loma Linda University, Loma Linda, CA, USA
[2]Department of Neurology, University of Erlangen-Nuremberg, Erlangen, Germany
[3]Department of Emergency Surgery, the First Affiliated Hospital of Soochow University, Suzhou, Jiangsu, China
[4]Department of Psychology, Loma Linda University, Loma Linda, CA, USA
[5]Department of Pediatrics, Loma Linda University, Loma Linda, CA, USA
[6]Department of Anesthesiology, Loma Linda University, Loma Linda, CA, USA
[7]Department of Neurosurgery, Loma Linda University, Loma Linda, CA, USA

*Anatol Manaenko and Peng Yang contributed equally to this work.

**Corresponding author:**
Jiping Tang, Department of Physiology & Pharmacology, School of Medicine, Loma Linda University, 11041 Campus St, Loma Linda, CA 92350, USA.
Email: jtang@llu.edu

bundles called stress fibers.[6] Stress fibers anchor to adherens junctions on the membranes of neighboring endothelial cells.[7] Under stress, the contraction of stress fibers results in the formation of intercellular gaps between endothelial cells, increasing the permeability of the BBB.[7]

The platelet-derived growth factor receptors (PDGFRs) are a possible trigger of the BBB dis-integrity. PDGFRs exist in two isoforms (α and β) and are expressed in all cells of the neurovascular unit, including endothelial cells.[8] While the detrimental role of the α-isoform in the development of secondary brain injury after stroke has been established,[9,10] the role of the β-isoform is controversial. Some studies suggest that PDGFR-β signaling is crucial for maintaining BBB integrity and tissue repair,[11] and others demonstrate that PDGFR-β activation causes fibrosis after brain injury[12] and stress fiber formation.[13,14]

One of the possible mechanisms that PDGFR-β activation contributes to BBB disruption is formation of stress fibers via activation of the cortactin/RhoA/LIMK pathway. Cortactin is a regulator of cytoskeleton and is downstream of PDGFR-β.[15] Upon activation, cortactin transmits a signal from PDGFR to RhoA and re-arranges the cytoskeleton.[16,17] RhoA is able to interact directly with LIM kinase (LIMK), another potent regulator of actin dynamics that is abundantly expressed in the CNS.[18–20] There are clear indications that F-actin accumulation and stress fiber formation are critically dependent on the LIMK activation.[21]

After brain injury, the activation of RhoA is accompanied by BBB disruption, and inhibition of RhoA preserves BBB after ICH.[22,23] Even without stroke, activation of RhoA in animals increases BBB permeability.[24] However, the effects of stroke on the activation of cortactin or LIMK and the consequences of this activation have not been evaluated yet. In this study, we tested the hypothesis that ICH induces formation of stress fibers triggered by activation of PDGFR-β that is mediated via the cortactin-RhoA-LIMK pathway. We postulated that stress fiber formation causes degradation of adherens/tight junction and consequently disruption of BBB. Most importantly, we tested whether PDGFR-β inhibition counteracts the effects of BBB disruption by ICH thus presenting itself as a potential therapy for ICH patients (Figure 1).

## Materials and methods

### Animals

A total of 208 male CD1 mice (eight-week-old, weight 30 g ± 5 g; Charles River, Wilmington, MA) were housed in a vivarium for a minimum of three days before surgery with a 12-h light/dark cycle and ad libitum access to food and water. All procedures in this study were approved by the Institutional Animal Care and Use Committee at Loma Linda University and comply with the National Institutes of Health's Guide for the Care and Use of Laboratory Animals, and the manuscript adheres to the ARRIVE (Animal Research: Reporting of In Vivo Experiments) guidelines for reporting animal experiments. Animals were randomly divided into different experimental groups. Animals, which died before final assessment, were replaced. There were no significant differences in the mortality rate between the different experimental groups.

### ICH mouse model

Experimental ICH was induced by intrastriatal injection of bacterial collagenase. We adopted the collagenase-induced ICH model in mice as previously described.[9] Briefly, mice were anesthetized with ketamine (100 mg/kg) and xylazine (10 mg/kg, intraperitoneal (I.P.) injection) and positioned prone in a stereotaxic head frame. An electronic thermostat-controlled warming blanket was used to maintain the core temperature at 37°C. The calvarium was exposed by a midline scalp incision from the nasion to the superior nuchal line, and the skin was retracted laterally. With a variable speed drill (Fine Scientific Tools, Foster City, CA, USA) a 1 mm burr hole was made 0.9 mm posterior to bregma and 1.4 mm to the right of the midline. A 26-G needle on a Hamilton syringe was inserted with stereotaxic guidance 4 mm into the right deep cortex/basal ganglia at a rate 1 mm/min. The collagenase (0.075 units in 0.5 µl saline, VII-S; Sigma, St Louis, MO, USA) was infused into the brain at a rate of 0.25 µl/min over 2 min with an infusion pump (Stoelting, Wood Dale, IL, USA). The needle was left in place for an additional 10 min after injection to prevent the possible leakage of the collagenase solution. After removal of the needle, the incision was closed, and the mice were allowed to recover. The sham operation was performed with needle insertion only.

### Drugs and RNAs administration

The PDGFR-β antagonist CP-673,451 (Selleckchem, Inc.) was dissolved in 0.1% DMSO and tested at two different concentrations: 15 and 50 mg/kg of body weight. The LIMK inhibitor, LIMKi 3 (Tocris Bioscience), was dissolved in 0.1% DMSO and tested at two different concentrations: 0.3 and 1 mg/kg of body weight. Both drugs were administered via I.P. injection in 500 µl. Vehicle-treated animals received equal amounts of 0.1% DMSO. Both PDGFR-β and

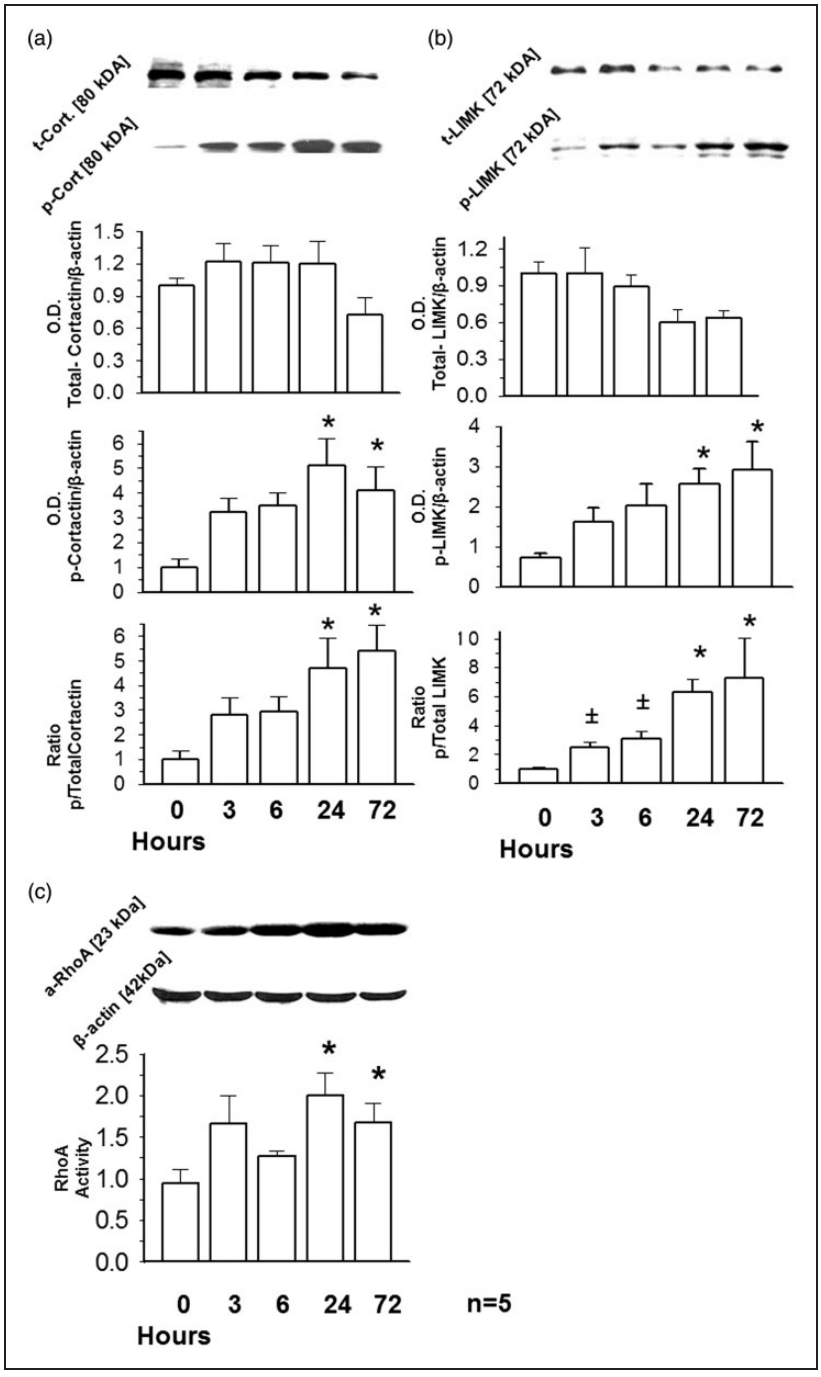


**Figure 1.** Time-dependent effects of ICH on cortactin-RhoA-LIMK pathway activation. Although ICH had no effect on expression of total cortactin, ICH significantly activated the cortactin and induced its phophorylation as early as 3 h after ICH (a). The difference to time point 0 became statistically significant 24 and 72 h after ICH. ICH had no effect on the expression of the total LIMK, but activated it, via phosphorylation of the protein, at 24 and 72 h after ICH (b). ICH activated RhoA 24 and 72 h after ICH (c). n = 5 per time point; *$p < 0.05$ vs. time point 0, ± $p < 0.05$ vs. time point 72 h. Values are expressed as mean ± SEM.

LIMKi antagonists were administrated 1 h after ICH induction

Both the PDGFR-β and cortactin small interfering RNA (si-RNA), as well as scrambled RNA (sc-RNA), were dissolved in sterile RNAse free resuspension buffer according to the manufacturer's instructions (OriGene). They were administrated via intraventricular injection (i.c.v.) to the right hemisphere twice (24 h prior to and 24 h after ICH) at 0.9 mm and 3.3 mm lateral from bregma. Si-RNA or sc-RNA (100 pmol)

was delivered in 2 µl with a Hamilton syringe over 2 min. The needle was left in place for an additional 5 min after injection to prevent possible leakage and then slowly withdrawn over 4 min. After the needle was removed, the burr hole was sealed with bone wax, the incision was closed with sutures, and the mice were allowed to recover. Vehicle-treated animals received an injection of suspension buffer. Recombinant PDGF-D (Abcam) was injected into the right basal ganglia of naïve mice (200 ng/2 µl PBS per mouse) using the same coordinates as the collagenase injections.

## Evaluation of BBB permeability and hematoma volume

*Evaluation of BBB permeability.* BBB permeability was evaluated by brain water content measurement and the Evans Blue assay. For brain water content measurement, the dry/wet method was used. Briefly, mice were euthanized under deep anesthesia. Brains were removed immediately and divided into five parts: ipsilateral and contralateral basal ganglia, ipsilateral and contralateral cortex, and cerebellum. The cerebellum was used as an internal control for brain water content. Tissue samples were weighed on an electronic analytical balance (model AE 100; Mettler Instrument Co., Columbus, OH, USA) to the nearest 0.1 mg to obtain the wet weight. The tissue was then dried at 100°C for 24 h to determine the dry weight. Brain water content (%) was calculated as [(wet weight – dry weight)/wet weight] × 100.

The Evans Blue assay was conducted by injecting I.P. a 2% solution of Evans Blue in normal saline (4 ml/kg of body weight), and the stain was then allowed to circulate for 3 h.[25] Afterwards, the mice were transcardially perfused with 100 ml of ice-cold PBS, the brain tissue was removed and divided into right and left hemispheres, frozen in liquid nitrogen, and stored at (−80°) C until analysis. The samples were homogenized in 1100 µl of PBS, sonicated and centrifuged (30 min, 15,000 rcf, 4°C). The supernatant was collected in aliquots. To each 500 µl aliquot, an equal amount of 50% trichloroacetic acid was added, incubated over night at 4°C, and then centrifuged (30 min, 15,000 rcf, 4°C). Evans Blue stain was measured by spectrophotometer (Thermo Spectronic Genesys 10 UV, Thermo Fischer Scientific Inc., Waltham, MA, USA) at 610 nm and quantified according to a standard curve. The results are presented as (µg of Evans Blue stain)/(g of tissue).

*Evaluation of hematoma value (hemoglobin assay).* Initially, a standard curve was obtained using a "virtual" model of hemorrhage. Brain tissue was obtained from naive mice subjected to complete transcardial perfusion to remove intravascular blood. Incremental volumes of homologous blood (0, 2, 4, 8, 16, and 32 µl) were added to each brain tissue sample with PBS to reach a total volume of 1100 µl, followed by homogenization for 30 s, sonication on ice for 1 min, and centrifugation at 15,000 r/min for 30 min (4°C). Drabkin's reagent (0.4 ml, Sigma) was added to 0.1 ml supernatant aliquots and allowed to stand for 15 min at room temperature. Optical density was measured and recorded at 540 nm with a spectrophotometer (Thermo Spectronic Genesys 10 UV, Thermo Fischer Scientific Inc., Waltham, MA, USA). These procedures yielded a linear relationship between measured hemoglobin concentrations in perfused brain and the volume of added blood.

For hematoma evaluation, supernatant was collected as described above (see evaluation of BBB permeability). For standard curve generation, Drabkin's reagent (0.4 ml, Sigma) was added to 0.1 ml supernatant aliquots and allowed to stand for 15 min at room temperature. Optical density was measured and recorded at 540 nm with a spectrophotometer (Thermo Spectronic Genesys 10 UV, Thermo Fischer Scientific Inc., Waltham, MA, USA)

## Neurobehavioral function test

Neurological scores were assessed by an independent researcher blinded to the procedure 23 and 71 h after ICH as previously described.[25] Two tests were used to evaluate neurological deficits: (1) The modified Garcia test, in which mice were given a score ranging from 0 to 21. The scoring system consists of seven tests (spontaneous activity, axial sensation, vibrissae proprioception, limb outstretching, lateral turning forelimb walking and climbing), with possible scores of 0–3 (0 = worst; 3 = best) for each. 2) The limb placement test, in which the animals were held by their trunk positioned parallel to a table top and slowly moved up and down, allowing the vibrissae on one side of the head to brush along the table surface. Refractory placements of the impaired (left) forelimb were evaluated, and a score was calculated as the number of successful forelimb placements out of 10 consecutive trials.

For long-term evaluation of spatial learning, a Morris Water Maze test was employed as described in our previous publication.[26]

## Sample preparation, Western blot and RhoA activity evaluation

Mice were perfused transcardially with 40 ml of cold PBS. Hemispheres were isolated and stored at (−80°C) until analysis.

*Western blot analysis.* Protein extraction and Western blots were performed according to the manufacturer's recommendation. Whole-cell lysates were obtained by gently homogenizing in RIPA lysis buffer (Santa Cruz Biotechnology, Inc., sc-24948) and centrifuging (14,000 *g* at 4°C for 30 min). The supernatant of the extract was collected, and the protein concentration was determined using a detergent compatible assay (Bio-Rad, Dc protein assay). Equal amounts of protein (50 μg) were loaded and subjected to electrophoresis on an SDS-PAGE gel. After being electrophoresed and transferred to a nitrocellulose membrane, the membrane was blocked and incubated with the primary antibody overnight at 4°C. Following antibodies were used: For an internal control, the same membrane was probed with an antibody against β-actin (Santa Cruz, 1:1000) after being stripped. Secondary antibodies (Santa Cruz Biotechnology) were incubated for 1 h at room temperature. Immunoblots were then probed with an ECL Plus chemiluminescence reagent kit (Amersham Biosciences, Arlington Heights, IL) and visualized with an imaging system (Bio-Rad, Versa Doc, model 4000). Data were analyzed using Image J software.

*Evaluation of RhoA activity.* RhoA activity was evaluated using a commercially available kit (Cytoskeleton Inc., Denver Co.). Two equal aliquots of each sample were taken. One aliquot was processed according to the manufacturer's recommendations and used for RhoA activity evaluation. The second aliquot was probed with an antibody against β-actin for the loading control.

### *Immunofluorescence study*

Seventy-two hours after ICH, the mice were perfused under deep anesthesia with cold phosphate-buffered saline (PBS, pH 7.4), followed by infusion of 10% paraformaldehyde. Brains were then removed and fixed in formalin at 4°C overnight. Samples were then dehydrated with 30% sucrose in phosphate-buffered saline (PBS, pH 7.4), and the frozen coronal slices (10 μm thick) were then sectioned using a cryostat (CM3050S; Leica Microsystems). Immunofluorescence was performed as previously described.[2] Briefly, samples were incubated with phospho-LIMK antibody (1:50, Abcam) at room temperature for 1 h. Afterward samples were washed three times with PBS and incubated with the secondary antibody (1:1000) in a cocktail with Alexa Fluor-phalloidin (100 nM, Cytoskeleton, Inc.). The slides were viewed and images were taken using LAS X software with a Leica DMi 8 fluorescence microscope (Leica Microsystems, Germany).

### *Statistics*

Analysis was performed using SigmaStat software, and data are expressed as mean ± standard error of the mean. Statistical differences were analyzed with one-way analysis of variance (ANOVA) followed by Fisher LSD Method. Statistical significance was defined as $p < 0.05$.

## Results

### *Mortality*

A total of 16 animals died before the end point as listed in the following:

24-h study: sham (N = 0), vehicle (N = 2), CP 673,451 (15 mg/kg) (N = 1), LIMKi (0.3 mg/kg) (N = 1), CP 673,451 (50 mg/kg) (N = 1).
72-h study: sham (N = 0), vehicle (N = 3), CP 673,451 (15 mg/kg) (N = 2), LIMKi (0.3 mg/kg) (N = 1), CP 673,451 (50 mg/kg) (N = 1), LIMKi (1.0 mg/kg) (N = 1).
28-day study: sham (N = 0), vehicle (N = 2), CP 673,451 (50 mg/kg) (N = 1).

The mortality (7.7%) of ICH animals was calculated and no statistical difference was obtained between experimental groups in this study.

### *ICH activated cortactin-LIMK pathway*

ICH did not affect the expression of total cortactin or LIMK, induced, however, phosphorylation forms of these proteins at 24 and 72 h after ICH (Figure 1(a) and (b)). At the same time points, activation of RhoA (Figure 1(c)) was observed.

### *ICH caused degradation of adherens/tight junction proteins*

ICH caused degradation of the adherens junction protein VE-cadherin at 3, 24, and 72 h (Supplemental Figure 2(a)). Significant degradation of tight junction proteins, occludin and claudin-3 was observed 72 h after ICH (Supplemental Figure 2(b) and (c)).

### *PDGFR-β inhibition attenuated ICH-induced disruption of BBB and improved neurological function, without having an effect on the hematoma volume*

No toxic effect of the PDGFR-β inhibition was observed in this study.

A collagenase injection at 24 h resulted in a significant elevation of brain water content in the ipsilateral basal

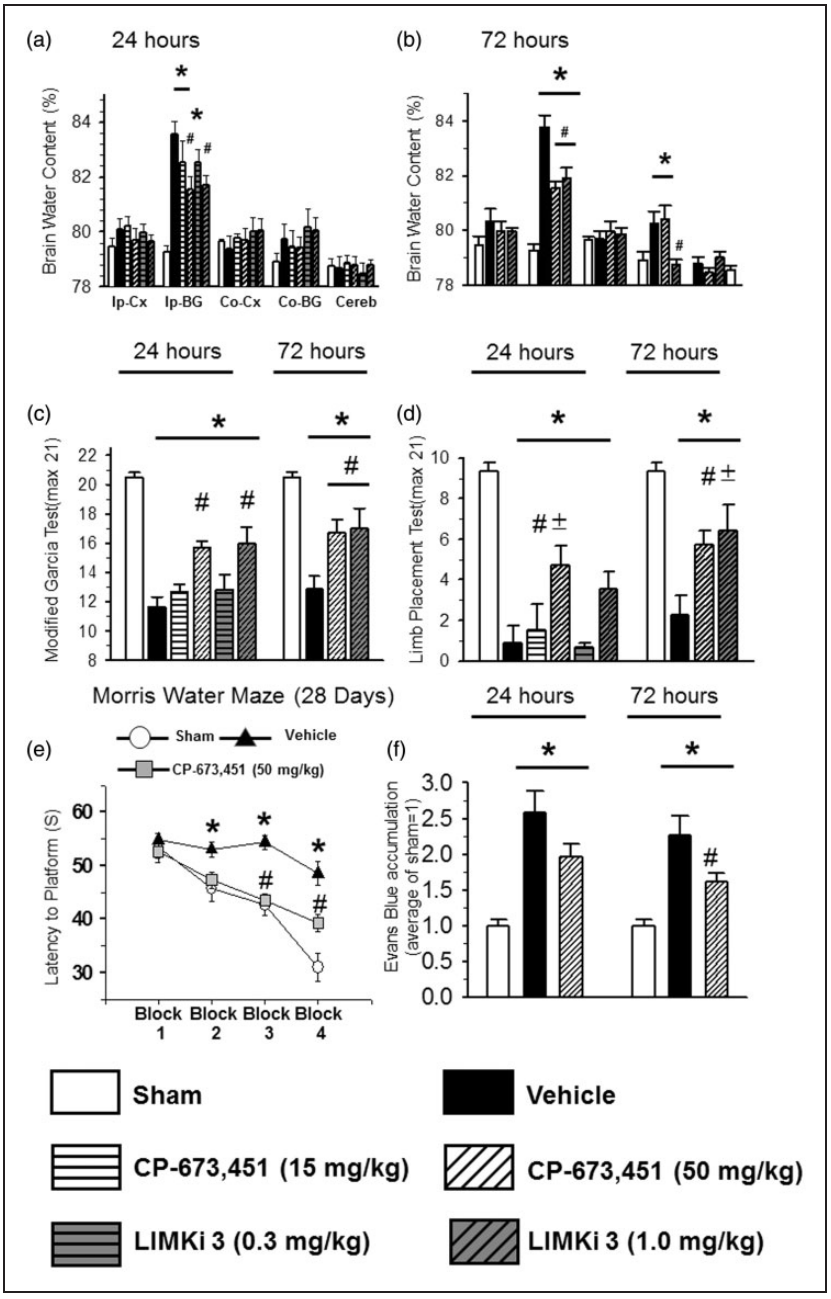


**Figure 2.** PDGFR-β and LIMK inhibition preserved BBB integrity and improved neurological functions after ICH. Collagenase injection caused significant increase of brain water content in the ipsilateral basal ganglia of ICH-animals (n = 7) compared to sham-operated animals (n = 6) at both 24 and 72 h after ICH (a and b). Although a low concentration of either PDGFR-β or LIMK, the inhibitor (n = 6) showed only tendency to attenuate the ICH-induced brain edema, a high concentration of inhibitors (n = 7), administrated 1 h after ICH, significantly reduced this parameter both at 24 (a) and at 72 (b) h after ICH. PDGFR-β or LIMK inhibition improved neurological function according to performance on the modified Garcia (c) and limb placement (d) tests. In the long-term study, we observed significant impairment of spatial learning in ICH (n = 9) compared to sham-operated animals (Morris Water Maze Test, (e)). High concentration of PDGFR-β inhibitor (n = 8) improved spatial learning of ICH animals 28 days after ICH (e). Compared to sham animals (n = 6), ICH-induced disruption of BBB resulted in significant accumulation of Evans Blues stain in the ipsilateral hemisphere of ICH animals (24 h n = 6, 72 h n = 7) (f).

Ip: ipsilateral; Cont: contralateral; Cx: Cortex; BG: basal ganglia; Cerebel: cerebellum.*$p < 0.05$ vs. sham, #$p < 0.05$ vs. vehicle, ±$p < 0.05$ vs. low concentration. Values are expressed as mean ± SEM.

ganglia of ICH (collagenase injected) animals compared to sham-operated (needle trauma) animals ($79.26 \pm 0.25\%$ vs. $83.55 \pm 0.49\%$, respectively, $p < 0.01$ Figure 2(a)). While low concentrations (15 mg/kg) of the PDGFR-β inhibitor CP-673,451 showed only a tendency to decrease ICH-induced increases of brain water content, the high concentration (50 mg/kg) significantly reduced post-ICH brain edema ($83.55 \pm 0.79$ vs. $81.55 \pm 0.5$; $p = 0.012$ Figure 2(a)). Seventy-two hours after ICH, we observed an increase in brain water content in both the ipsilateral and contralateral basal ganglia of ICH compared to the sham animals (ipsilateral $83.69 \pm 0.47$ vs. $79.26 \pm 0.25$ $p < 0.001$; contralateral $80.73 \pm 0.33$ vs. $78.92 \pm 0.3$, respectively $p = 0.005$, Figure 2(b)). High concentrations of CP-673,451 decreased brain edema in the ipsilateral ($81.53 \pm 0.24$, $p < 0.001$) and showed a tendency but not significant to decrease brain water content in the contralateral basal ganglia ($p = 0.546$) (Figure 2(b)).

In agreement with that, PDGFR-β inhibition improved ICH-impaired neurological function as evaluated by the modified Garcia test (Figure 2(c) left panel vehicle vs. CP-673,451 (50 mg/kg), $p = 0.004$) and limb placement tests (Figure 2(d) left panel, vehicle vs. CP-673,451 (50 mg/kg), $p = 0.006$). Amelioration of ICH-induced brain edema was accompanied with improvement of neurological function evaluated 72 h after ICH (Figure 2(c) and (d) right panel, vehicle vs. CP-673,451 (50 mg/kg): modified Garcia, $p = 0{,}002$: Limb Placement test $p = 0.004$).

In long-term study, we observed significant impairment of spatial learning of ICH compared to vehicle animals evaluated on Morris Water Maze Test (Figure 2(e)). CP-673,451 (50 mg/kg) ameliorated ICH-induced impairment of spatial learning (Figure 2(e)).

The Evans Blue assay revealed significant BBB disruption after ICH. The accumulation of Evans Blue stain in the ipsilateral hemisphere of ICH compared to the sham animals was observed both at 24 and 72 h after ICH induction (Figure 2(f)). PDGFR-β inhibition significantly decreased ICH-induced stain accumulation at 72 h and showed a tendency to decrease stain accumulation at 24 h after ICH (Figure 2(f)).

PDGFR-β inhibition did not affect hematoma volume (data not shown).

### *PDGFR-β knock-down attenuated both ICH-induced activation of cortactin-RhoA-LIMK pathway and degradation of adherens/tight junction proteins*

To rule out non-specific effects of the PDGFR-β inhibitor, we used si-RNA for the receptor to investigate the molecular mechanisms that underlie the protective effects of the receptor inhibition. Administration (i.c.v.) of si-RNA decreased the expression of the receptor (Figure 3(a), vehicle vs. si-RNA $p < 0.001$). This was accompanied by attenuating activation of the cortactin-RhoA-LIMK pathway (Figure 3(b) vehicle vs. si-RNA pCort $P = 0.039$, aRhoA $= 0.02$, pLIMK $p < 0{,}001$) and by decreased degradation of adherens/tight junction proteins (Figure 3(c), vehicle vs. si-RNA, Ve-Cadherin $p = 0.017$, Occludin $p = 0.002$, Claudin 3 $p = 0.002$). Administration of sc-RNA did not affect these parameters.

### *Knock-down of PDGFR-β downstream, cortactin attenuated both ICH-induced activation of RhoA-LIMK pathway and degradation of adherens/tight junction proteins*

Administration (i.c.v.) of cortactin si-RNA decreased the expression of this protein (Figure 4(a), vehicle vs. si-RNA $p = 0.021$). Decreased expression of the cortactin corresponded both with diminished activation of the RhoA-LIMK pathway (Figure 4(b), vehicle vs. si-RNA: pLIMK $p = 0{,}031$, RhoA $p < 0.001$) and with decreased degradation of adherens/tight junction proteins (Figure 4(c), vehicle vs. si-RNA: Occludin $p < 0.001$). Administration of sc-RNA did not affect these parameters.

### *LIMK inhibition preserved BBB and attenuated neurological deficits after ICH*

Compared to vehicle-treated animals, animals treated with high concentrations of the LIMK inhibitor LIMKi 3 (1 mg/kg) had significantly decreased brain water content at both 24 and 72 h after ICH (24 h: $83.271 \pm 0.412$ vs. $81.730 \pm 0.34$, $p = 0.007$; 72 h: $83.77 \pm 0.44$ vs. $81.92 \pm 0.37$, $p = 0.003$; vehicle vs. treatment respectively (Figure 2(a) and (b)). Correspondingly, high concentrations of LIMKi 3 significantly improved post-ICH neurological functions as evaluated by the modified Garcia (vehicle vs. treatment 24 h $p = 0.002$, 72 h $p = 0.02$) and Limb placement tests (vehicle vs. treatment 24 h $p = 0.011$, 72 h $p = 0.003$) (Figure 2(c) and (d)).

Seventy-two hours after ICH, a high concentration of LIMKi 3 decreased ICH-induced phosphorylation of LIMK in treated compared to untreated animals (Figure 5(a), $p = 0.008$). This was accompanied by attenuation of adherens/tight junction protein degradation (Figure 5(b) vehicle vs. treatment $p = 0.021$).

### *The endogenous PDGFR-β agonist PDGF-D induced activation of cortactin-RhoA-LIMK pathway and degradation of adherens/tight junction proteins in naïve animals*

Seventy-two hours after injection of the recombinant PDGF-D into the brains of naïve animals, we observed

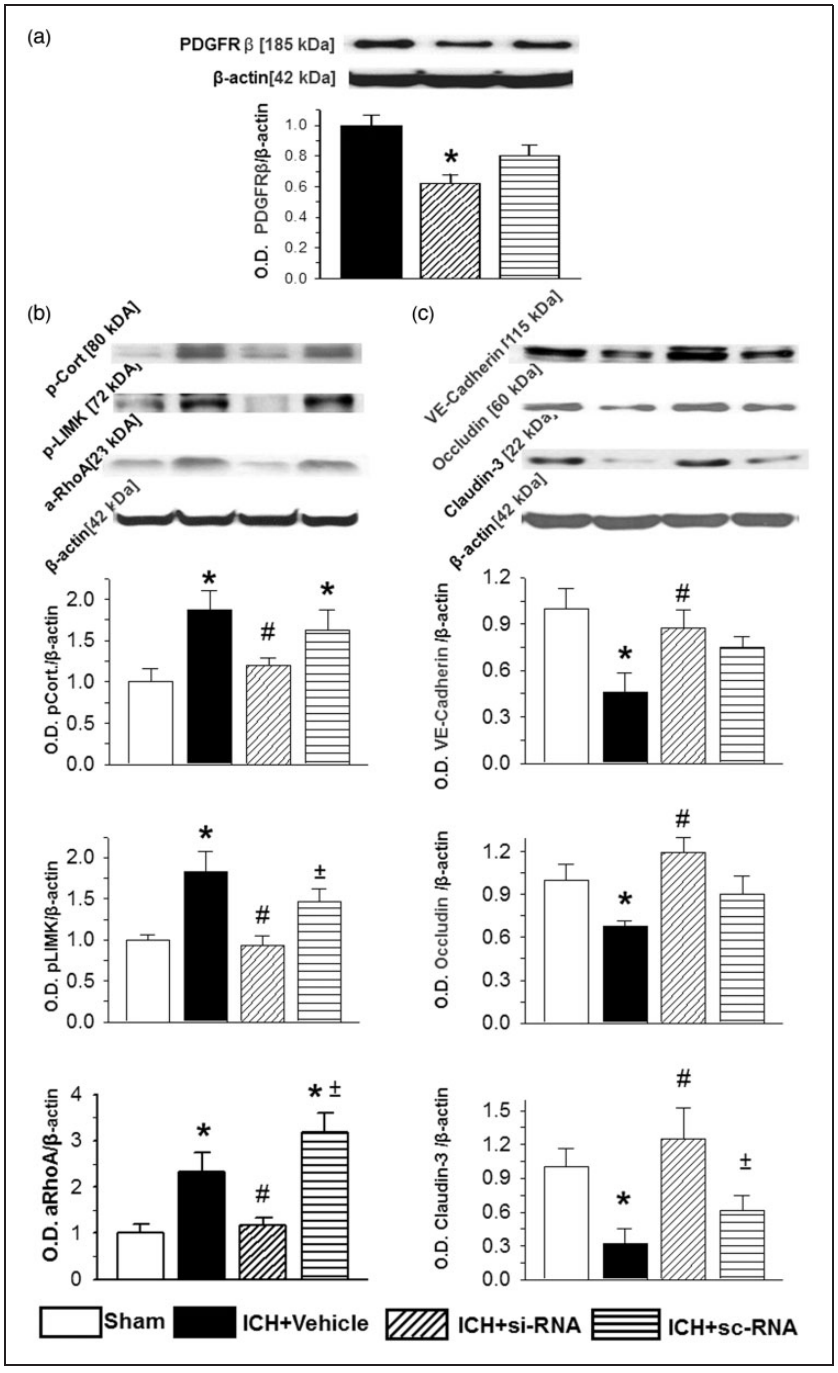


**Figure 3.** Knock-down of PDGFR-β attenuated ICH-induced activation of the cortactin-RhoA-LIMK pathway and preserved BBB. I.c.v. administration of si-RNA for PDGFR-β (si-RNA) significantly decreased expression of the receptor when evaluated 72 h after ICH. Sc-RNA administration did affect the receptor expression (sc-RNA) (a). Decrease of the PDGFR-β expression was accompanied with significant attenuation of ICH-induced activation of the cortactin-RhoA-LIMK pathway (b) and resulted in preservation of adherens/tight junction proteins (c) 72 h after ICH. ($n = 6$ per group, $^{*}p < 0.05$ vs. sham, $^{\#}p < 0.05$ vs. vehicle, $\pm\, p < 0.05$ vs. scrambled RNA). Values are expressed as mean ± SEM.

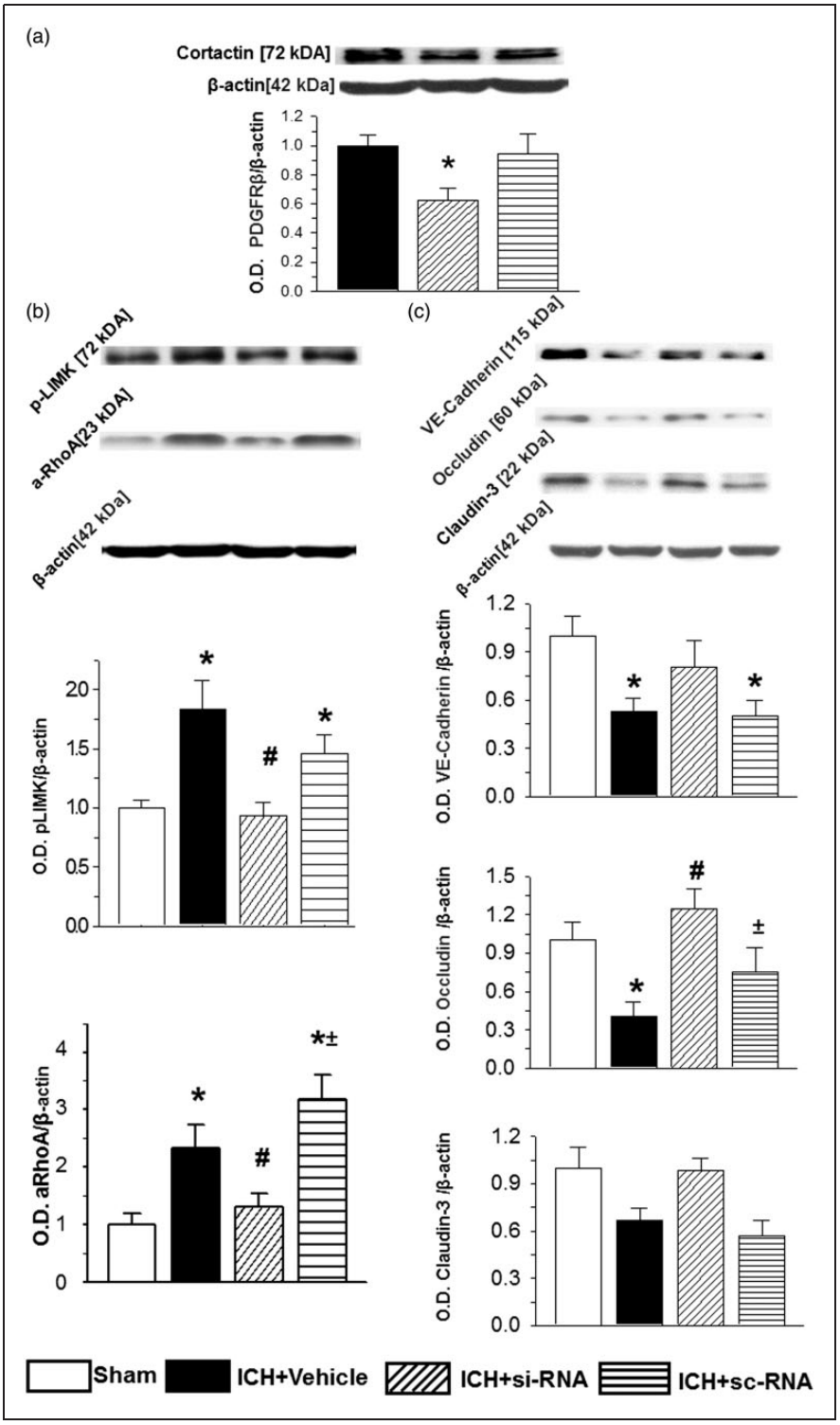


**Figure 4.** Knock-down of PDGFR-β downstream, cortactin, attenuated ICH-induced activation of the RhoA-LIMK pathway and preserved BBB. I.c.v. administrations of si-RNA for cortactin (si-RNA) significantly decreased expression of the protein 72 h after ICH. Scrambled RNA administration did affect the receptor expression (sc-RNA) (a). At 72 h, the decrease of the cortactin was accompanied with significant attenuation of ICH-induced activation of RhoA-LIMK pathway (b) and resulted in preservation of adherens/tight junction proteins (c). n = 6 per group, * $p < 0.05$ vs. sham, $^{\#}p < 0.05$ vs. vehicle, $\pm\, p < 0.05$ vs. scrambled RNA. Values are expressed as mean ± SEM.

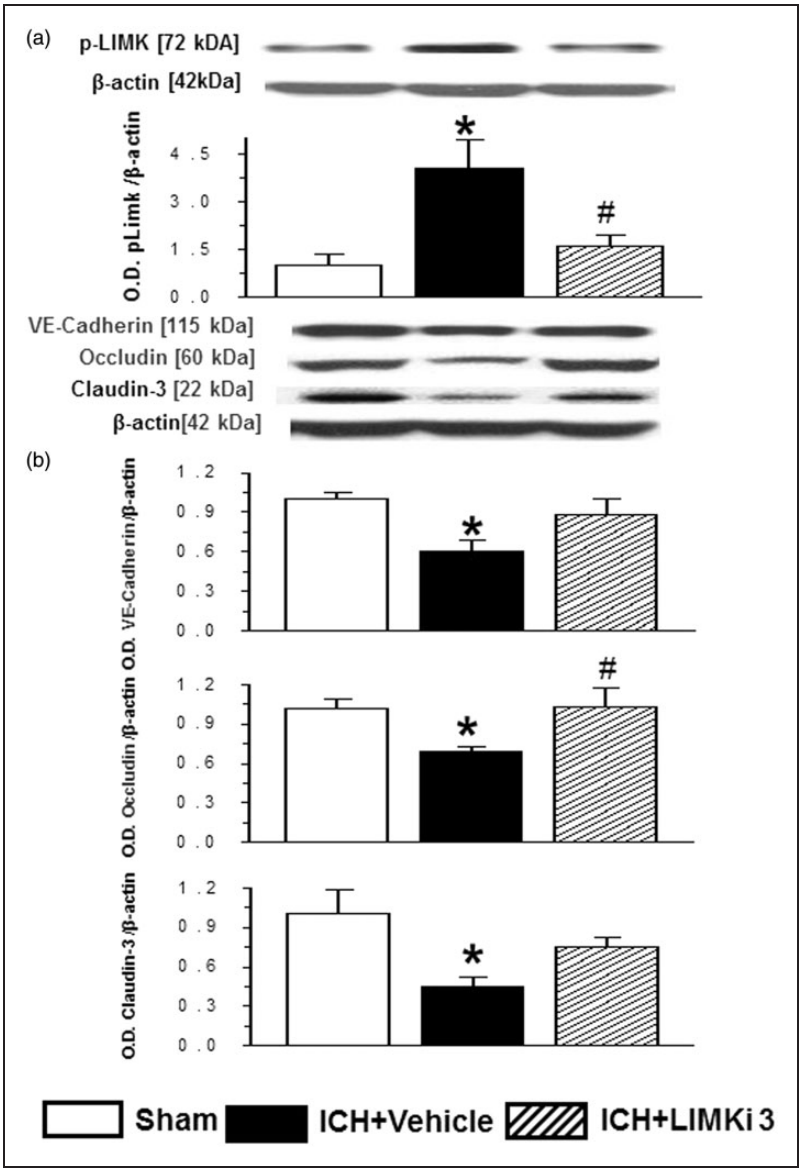


**Figure 5.** LIMK inhibitor, LIMKi 3, both reduced ICH-induced phosphorylation of LIMK and preserved BBB as well as improved post ICH neurological function. High concentration of LIMKi 3 (1 mg/kg n = 6) attenuated ICH-induced LIMK activation (ICH n = 6) evaluated 72 h after ICH (a) and consequently attenuated ICH degradation of adherens/tight junction proteins (n = 6 per group) at the same time point (b). $^{*}p < 0.05$ vs. sham, $^{\#}p < 0.05$ vs. vehicle, $\pm\, p < 0.05$ vs. scrambled RNA. Values are expressed as mean ± SEM.

significant activation of the RhoA-LIMK pathway (sham vs. PDGF D: pCortactin $p = 0.002$, pLIMK $p = 0.008$) and a tendency to activate cortactin ($p = 0.071$; Figure 6(a)). The activation of the pathway resulted in degradation of VE-cadherin ($p = 0.012$) and occludin ($p = 0.041$) (Figure 6(b)).

### *ICH and PDGF-D induced formation of stress fibers, inhibition of PDGFR-β, cortactin or LIMK resulted in decreased stress fiber formation after ICH*

Immunostaining revealed that ICH caused a dramatic increase of phalloidin-positive cells (Figure 7) in ICH versus sham-operated animals, indicating stress fiber formation. Most of the stress fibers were positive for phosphorylated LIMK (pLIMK), demonstrating the importance of pLIMK in the formation of stress fibers. Inhibition of the proposed pathway considerably decreased the amount of both stress fiber and pLIMK-positive cells. Sc-RNA did not affect this parameter. Recombinant PDGF-D increased the number of stress fibers compared to sham animals.

Morphology of F-actin stress fiber and their colocalization with pLIMK in the higher magnification is demonstrated in Supplemental Figure 3.

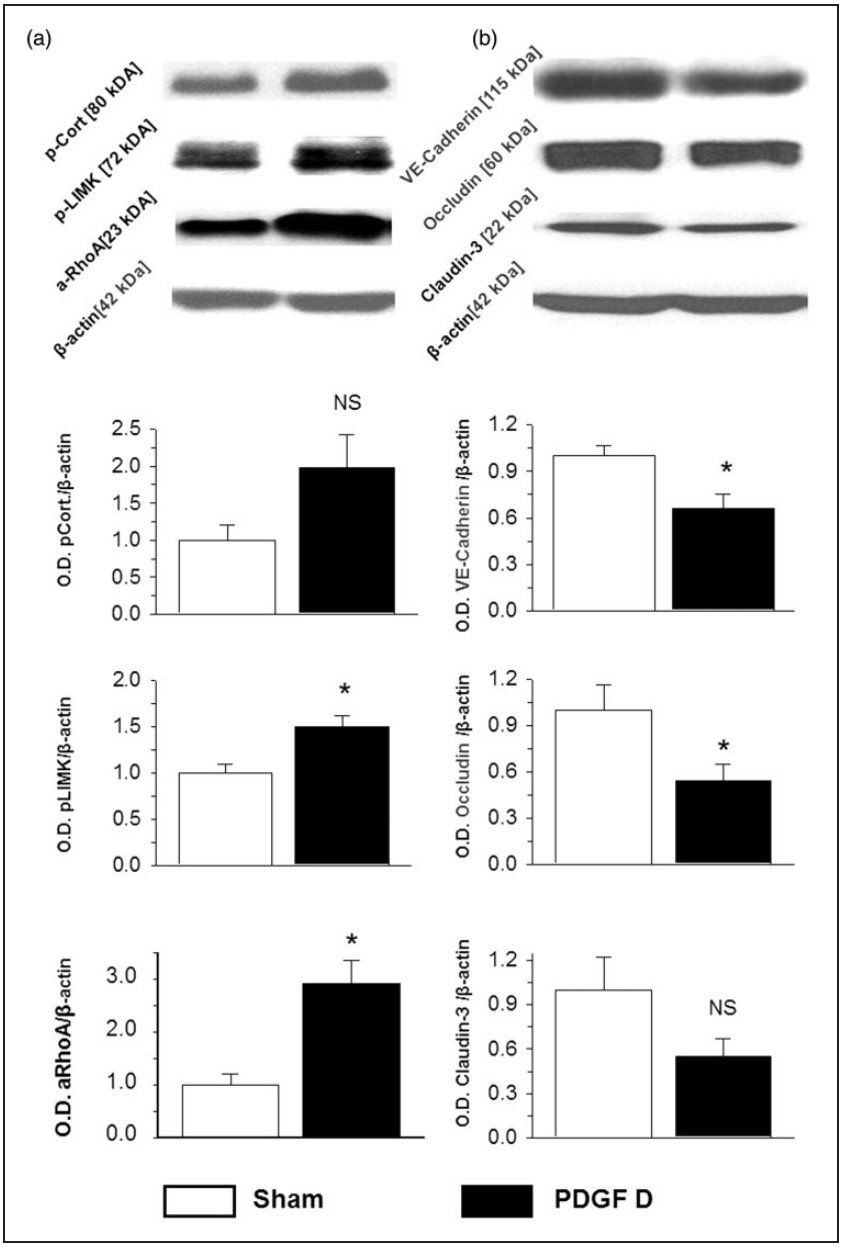


**Figure 6.** The endogenous agonist of PDGFR-β, PDGF-D, partly induced activation of the RhoA-LIMK pathway and degradation of adherens/tight junction proteins; 72 h after administration of PDGF-D into the basal ganglia of naïve animals, partial activation of the cortactin-RhoA-LIMK pathway was observed (a). That was accompanied with degradation of adherens/tight junction proteins (b). n = 6 per group, $^{*}p < 0.05$ vs. sham, $^{\#}p < 0.05$ vs. vehicle, $\pm\, p < 0.05$ vs. scrabble RNA. Values are expressed as mean ± SEM.

## Discussion

In the present study, we investigated for the first time the effects of ICH on stress fiber formation. We demonstrated that (1) ICH induced formation of stress fibers that were associated with degradation of BBB components, BBB disruption, and the consequent development of brain edema, and (2) these post-ICH events were mediated, at least partly, by PDGFR-β activation via the cortactin/RhoA/LIMK pathway. Furthermore, we established that inhibition of the PDGFR-β pathway is beneficial and protects BBB integrity after ICH.

We demonstrated previously that ICH induced a time-dependent increase of both PDGF production and PDGFR expression.[9] The expression of PDGFR-β increased at 6 h, peaked at 12 h, remained upregulated at 24 h, and returned to the baseline 72 h after ICH. In the present study, we demonstrated that ICH caused rapid activation of cortactin/RhoA/LIMK, in a manner similar to PDGF-β activation. Compared to

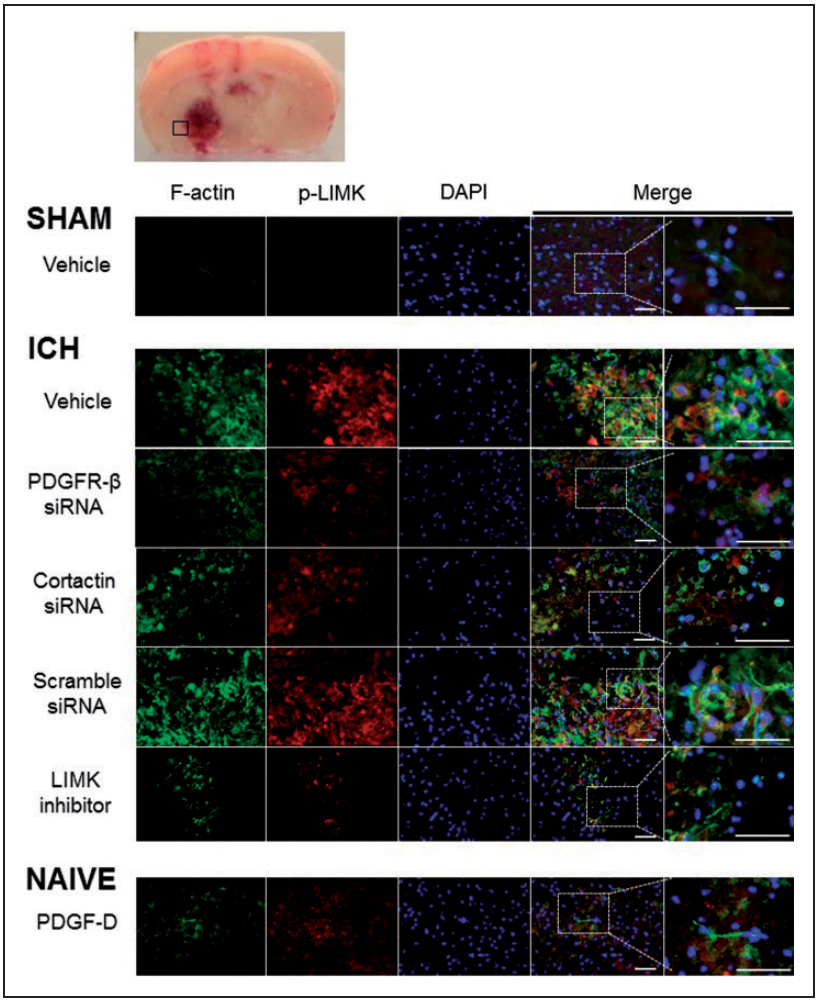


**Figure 7.** ICH-induced activation of LIMK and intensive formation of F-actin stress fibers. Stress fibers were visualized with Alexa Fluor-phalloidin kit. Phalloidin had a high affinity to the F-actin and stress fibers appeared green (column "F-actin"). Cells positive for the activated LIMK appeared red (column "*p*-LIMK"). The ICH significantly increased the number of both activated LIMK-positive (red) and phalloidin-positive (green) cells as well as double-positive phalloidin/pLIMK stress fibers (first column "Merge"). While treatment with siRNA for both PDGFR-β and cortactin as well as LIMK inhibition resulted in fewer LIMK-positive stress fibers, scrambled RNA did not have such effect. Injection of PDGF-D into the brain of naïve animals resulted in activation of LIMK and formation of stress fiber compared to sham-operated animals. The second "Merge" column showed the detailed morphology of pLIMK-positive stress fiber in more details.

baseline, these proteins became activated 6 h after ICH. The difference from baseline became statistically significant at 24 h and remained upregulated 72 h after ICH. RhoA activation was observed at the same time points, consistent with the previous study.[23]

Next, we investigated whether activation of cortactin/RhoA/LIMK would be accompanied with degradation of BBB components as a consequence of stress fiber formation. The BBB's permeability is regulated by adherens junctions, which in turn, play an important role in stabilizing tight junctions.[27] There are indications that pathophysiological conditions activate endothelia, changing endothelial cytoskeletons in the BBB. This process forms stress fibers that create gaps between intact endothelial cells and promote tissue edema.[6]

We confirmed that activation of the proposed pathway leads to time-dependent degradation of adherens/tight junction proteins. We investigated the effects of ICH on VE-cadherin, occludin, and claudin-3. VE-cadherin is an endothelial-specific cell-to-cell adhesion protein in the adherens junction that is essential for endothelial cell permeability.[28] Genetic or pharmacologic inactivation of the VE-cadherin decreases vascular integrity and facilitates transmigration of leukocytes.[29] Moreover, decreased VE-cadherin expression was accompanied by increased permeability of the BBB to Evans Blue stain in different models of brain injury.[30]

VE-cadherin directly controls expression of the tight junction protein claudin-5.[31] The degradation of claudin-5 after ICH has been demonstrated previously.[32] Claudin-3, another protein of the claudin family, is expressed in brain endothelia[33] and its degradation compromises BBB under pathological conditions.[34] Additionally, we investigated the time-dependent effects of ICH on occludin, another tight junction protein playing a key role in BBB integrity.[35] In our study, VE-cadherin degradation was detectable 24 and 72 h after ICH, and degradation of claudin-3 and occludin was detected 72 h after ICH.

The degradation of BBB proteins corresponded to the activation of the cortactin-RhoA-LIMK pathway after ICH. Importantly, we were able to demonstrate that ICH-induced degradation of the BBB components was accompanied by formation of stress fibers. We investigated this parameter 72 h after ICH, the time point of maximal degradation of adherent-tight junction proteins. For visualization of stress fibers, we used phalloidin staining. Phalloidin, a bicyclic peptide with high affinity for F-actin, is commonly used to visualize F-actin stress fibers.[36] We observed a significant increase in phalloidin-positive cells in the brain after ICH, indicating endothelial activation and stress fiber formation.

Furthermore, we investigated whether inhibition of PDGFR-β would decrease ICH-induced stress fiber formation and BBB disruption, leading to improved neurological functions. For the PDGFR-β inhibition, we used a commercially available receptor antagonist, CP-673,451 that is a selective inhibitor of PDGFRs, having 10 fold more selectivity for the β-isoform as compared to its selectivity for the α-isoform of the receptor.[37] The drug concentrations used in this study were chosen according to previous publications. In agreement with prior reports, no toxic effect of the drug was observed.[37] We demonstrated that the inhibition of the receptor attenuated ICH-induced brain edema and improved ICH-impaired neurologic functions at both 24 and 72 h post-ICH. These findings agree with our previous study, demonstrating that a selective, si-RNA-induced, in-vivo knock-down of PDGFRβ, decreased brain water content and improved neurological functions 24 and 72 h after ICH.[38] Additionally, we investigated the effect of PDGFR-β inhibition on BBB integrity using the Evans Blue assay. Although PDGFR-β inhibition only slightly decreased the amount of Evans Blue stain in the brain at 24 h, PDGFR-β inhibition significantly decreased ICH-induced accumulation of the stain after 72 h that differed from the results of nonselective PDGFR inhibition.[9] We demonstrated previously that nonselective inhibition of both α and β isoform of the PDGFR by Gleevec was able to decrease Evan Blue stain accumulation both at 24 and at 72 h after ICH significantly.[9] Both brain water content and the Evans Blue assays are used to evaluate BBB integrity, the two approaches revealed different outcomes. While brain water content accounts for both cytotoxic and vasogenic brain edema, the Evans Blue assay evaluates permeability of BBB to high-molecular weight proteins, which is a sign of vasogenic brain edema. The mechanism of edema formation after ICH is not completely understood. Most of the investigators, however, postulate that both cytotoxic and vasogenic brain edema is present after ICH.[39]

Whereas cytotoxic edema is prominent in the early stages of ICH, vasogenic edema follows later with the disruption of BBB. Twenty-four hours after ICH, both cytotoxic and vasogenic edema are simultaneously present.

We previously demonstrated that ICH induced a quick activation of the PRGFRα isoform as early as 3 h after ICH. The activation peaked (6-fold compared to sham-operated animals) 6 h after ICH. Although PRGFRα remained activated 12 h after ICH, the activation declined rapidly (2.5 fold).[9] The β-isoform became activated more slowly. The activation of β-isoform peaked at 12 h and remained on the same level 24 h after ICH.[38] Nonselective inhibition of both PDGFR isoforms via Gleevec decreased ICH-induced increase of brain water content and Evan Blue stain accumulation 24 and 72 h after ICH and obviously attenuated the development of both cytotoxic and vasogenic form of brain edema at this time points.[9] At 24 h after ICH, the treatment that inhibits mostly the β-isoform of the receptor, was also able to attenuate the development of cytotoxic edema, evaluated by brain water content calculation (the molecular pathways underlying the receptor inhibition on cytotoxic brain edema remain to be investigated). That was, however, not sufficient for attenuation of vasogenic edema. We are postulating that at this time point (due to low affinity of our drug to the α-isoform of the receptor and only minor activation of β-isoform) CP-673,451 was unable to inhibit the receptor completely. The partly inhibition of the PDGFRs did not lead to the amelioration of the vasogenic edema in the early stage of ICH. However, in the time point of the maximal PDGFR-β activation (72 hours post ICH), the inhibition of the PDGFR via a β-isoform inhibitor (CP-673,451), resulted in amelioration of BBB disruption, and attenuation of vasogenic edema, as evaluated by Evans Blue. These facts let us to the conclusion that a further, a head-to-head, investigation of the advantages of nonselective vs. selective inhibition of the different PDGFR isoform need to be done.

There are the indications in the literature that PDGFR-β is a positive regulator of tissue repair and

angiogenesis after ischemic stroke.[40] The inhibition of the receptor might have undesirable effects and affect the post-ICH recovery process negatively. In order to investigate this option, we conducted a long-term study. Our results demonstrated that the receptor inhibition significantly improved neurological functions after ICH. We suggest therefore that the drug, used in the study did not have adverts effects on angiogenesis and recovery after ICH.

Although CP-673451, the PDGFR-β inhibitor used in this study, is 10-fold more selective for the β-isoform as compared to the α-isoform of the PDGFR, it is challenging to rule out effects of the drug on the α-isoform in an in vivo study. To determine the effects of the β-isoform, we used si-RNA for the PDGFR-β. I.c.v administration of the si-RNA decreased expression of PDGFR-β and diminished the amount of phalloidin-positive F-actin stress fibers. Furthermore, si-RNA for PDGFR-β significantly reduced ICH-induced activation of cortactin-RhoA-LIMK pathway and attenuated degradation of adherens/tight junction proteins.

To investigate the role of cortactin on the induction of stress fibers after ICH, we used si-RNA for cortactin. Similar to PDGFR-β, si-RNA for cortactin significantly decreased expression of the protein. This reduction was accompanied by deactivation of RhoA and LIMK, decreased number of stress fibers, and the stabilization of adherens/tight junction proteins.

To investigate the effects of LIMK inhibition, we used a commercially available inhibitor, LIMKi 3.[41] First, we established a dose-dependent response of the drug on ICH-induced elevation of brain water content and neurological deficits in the short-time study. The drug, at a dose of 1 mg/kg, decreased brain edema and improved neurological function 72 h after ICH. At 72 h, this dose of LIMKi 3 significantly attenuated ICH-induced LIMK phosphorylation in brain tissue, indicating that LIMKi 3 can penetrate the BBB after ICH and has effects on the CNS. The results of the Western blot study were confirmed by immunostaining, which also revealed a decrease of pLIMK-positive cells in ICH animals treated with LIMKi 3 – compared to vehicle-treated animals. The effects of LIMKi 3 on post-ICH LIMK phosphorylation were associated with fewer stress fibers and preservation of adherens-tight junction proteins.

Finally, we investigated whether the injection of recombinant PDGF-D into the brain of naïve animals would result in activation of the proposed pathway and in the degradation of BBB proteins. PDGF-D is the endogenous agonist of the PDGFRs. Although there are some indications that PDGF-D has some affinity for the α-isoform of the receptor,[42] most investigators consider PDGF-D as a selective agonist for the PDGFR-β isoform.[43] Accordingly, PDGF-D administration should primarily activate PDGFR-β. We demonstrated that PDGF-D administration increased the amount of stress fibers, which was accompanied by RhoA-LIMK activation and degradation of VE-cadherin/occludin.

The current study has limitations. The drug used in the study has not been approved for patients. Intraperitoneal administration of the drug is untypical for patient. It is, however, worth to mention that intraperitoneal administration is very common for in small animals.[44] The pharmacokinetic partially mimics oral administration in human patients.[45]

In conclusion, our findings suggest that PDGFR-β contributes, at least partly, to ICH-induced stress fiber formation, BBB impairment, and impairment of neurological functions via the cortactin-RhoA-LIMK pathway. PDGFR-β inhibition had no toxic side effects and did not increase mortality after ICH. Although the PDGFR-β inhibition was not able to completely prevent brain injury after ICH, it attenuated significantly ICH-induced brain injury and improved neurological function after ICH. Our results, however, demonstrated that targeting PDGFR-β signaling may pave the way for a new therapeutic strategy for ICH patients.

## Funding

The author(s) disclosed receipt of the following financial support for the research, authorship, and/or publication of this article: This study was supported by NIH P01 NS082184-01 to JHZ.

## Declaration of conflicting interests

The author(s) declared no potential conflicts of interest with respect to the research, authorship, and/or publication of this article.

## Authors' contributions

AM and PY worked on experimental design, conduction of the experiments and data analysis. AM drafted the manuscript. EB and DN conducted experiments. REH, AO, and WJP contributed in manuscript preparation. JHZ and JT worked on experimental design, data analysis, and manuscript preparation.

## Supplementary material

Supplementary material for this paper can be found at http://jcbfm.sagepub.com/content/by/supplemental-data

## References

1. Balami JS and Buchan AM. Complications of intracerebral haemorrhage. *Lancet Neurol* 2012; 11: 101–118.
2. Chen S, Yang Q, Chen G, et al. An update on inflammation in the acute phase of intracerebral hemorrhage. *Trans Stroke Res* 2015; 6: 4–8.
3. Merali Z, Leung J, Mikulis D, et al. Longitudinal assessment of imatinib's effect on the blood-brain barrier after ischemia/reperfusion injury with permeability MRI. *Trans Stroke Res* 2015; 6: 39–49.

4. Selim M and Sheth KN. Perihematoma edema: a potential translational target in intracerebral hemorrhage? *Transl Stroke Res* 2015; 6: 104–106.
5. Schlunk F and Greenberg SM. The pathophysiology of intracerebral hemorrhage formation and expansion. *Transl Stroke Res* 2015; 6: 257–263.
6. Adyshev DM, Dudek SM, Moldobaeva N, et al. Ezrin/radixin/moesin proteins differentially regulate endothelial hyperpermeability after thrombin. *Am J Physiol Lung Cell Mol Physiol* 2013; 305: L240–L255.
7. Millan J, Cain RJ, Reglero-Real N, et al. Adherens junctions connect stress fibres between adjacent endothelial cells. *BMC Biol* 2010; 8: 11.
8. Shih RH, Cheng SE, Hsiao LD, et al. Cigarette smoke extract upregulates heme oxygenase-1 via PKC/NADPH oxidase/ROS/PDGFR/PI3K/Akt pathway in mouse brain endothelial cells. *J Neuroinflammation* 2011; 8: 104.
9. Ma Q, Huang B, Khatibi N, et al. PDGFR-alpha inhibition preserves blood-brain barrier after intracerebral hemorrhage. *Ann Neurol* 2011; 70: 920–931.
10. Su EJ, Fredriksson L, Geyer M, et al. Activation of PDGF-CC by tissue plasminogen activator impairs blood-brain barrier integrity during ischemic stroke. *Nat Med* 2008; 14: 731–737.
11. Bell RD, Winkler EA, Sagare AP, et al. Pericytes control key neurovascular functions and neuronal phenotype in the adult brain and during brain aging. *Neuron* 2010; 68: 409–427.
12. Papke CL, Cao J, Kwartler CS, et al. Smooth muscle hyperplasia due to loss of smooth muscle alpha-actin is driven by activation of focal adhesion kinase, altered p53 localization and increased levels of platelet-derived growth factor receptor-beta. *Hum Mol Genet* 2013; 22: 3123–3137.
13. Stice LL, Forman LW, Hahn CS, et al. Desensitization of the PDGFbeta receptor by modulation of the cytoskeleton: the role of p21(Ras) and Rho family GTPases. *Exp Cell Res* 2002; 275: 17–30.
14. Theisen CS, Wahl JK 3rd, Johnson KR, et al. NHERF links the N-cadherin/catenin complex to the platelet-derived growth factor receptor to modulate the actin cytoskeleton and regulate cell motility. *Mol Biol Cell* 2007; 18: 1220–1232.
15. Gunning PW, Hardeman EC, Lappalainen P, et al. Tropomyosin – master regulator of actin filament function in the cytoskeleton. *J Cell Science* 2015; 128: 2965–2974.
16. Boyle SN, Michaud GA, Schweitzer B, et al. A critical role for cortactin phosphorylation by Abl-family kinases in PDGF-induced dorsal-wave formation. *Curr Biol* 2007; 17: 445–451.
17. Lai FP, Szczodrak M, Oelkers JM, et al. Cortactin promotes migration and platelet-derived growth factor-induced actin reorganization by signaling to Rho-GTPases. *Mol Biol Cell* 2009; 20: 3209–3223.
18. Park JB, Agnihotri S, Golbourn B, et al. Transcriptional profiling of GBM invasion genes identifies effective inhibitors of the LIM kinase-Cofilin pathway. *Oncotarget* 2014; 5: 9382–9395.
19. Yi R, Xiao-Ping G and Hui L. Atorvastatin prevents angiotensin II-induced high permeability of human arterial endothelial cell monolayers via ROCK signaling pathway. *Biochem Biophys Res Commun* 2015; 459: 94–99.
20. Gong C, Stoletov KV and Terman BI. VEGF treatment induces signaling pathways that regulate both actin polymerization and depolymerization. *Angiogenesis* 2004; 7: 313–321.
21. Thirone AC, Speight P, Zulys M, et al. Hyperosmotic stress induces Rho/Rho kinase/LIM kinase-mediated cofilin phosphorylation in tubular cells: key role in the osmotically triggered F-actin response. *Am J Physiol Cell Physiol* 2009; 296: C463–C475.
22. Fu Z, Chen Y, Qin F, et al. Increased activity of Rho kinase contributes to hemoglobin-induced early disruption of the blood-brain barrier in vivo after the occurrence of intracerebral hemorrhage. *Int J Clin Exp Pathol* 2014; 7: 7844–7853.
23. Huang B, Krafft PR, Ma Q, et al. Fibroblast growth factors preserve blood-brain barrier integrity through RhoA inhibition after intracerebral hemorrhage in mice. *Neurobiol Dis* 2012; 46: 204–214.
24. Yu Y, Qin J, Liu M, et al. Role of Rho kinase in lysophosphatidic acid-induced altering of blood-brain barrier permeability. *Int J Mol Med* 2014; 33: 661–669.
25. Manaenko A, Chen H, Kammer J, et al. Comparison Evans Blue injection routes: Intravenous versus intraperitoneal, for measurement of blood-brain barrier in a mice hemorrhage model. *J Neurosci Meth* 2011; 195: 206–210.
26. Hartman R, Lekic T, Rojas H, et al. Assessing functional outcomes following intracerebral hemorrhage in rats. *Brain Res* 2009; 1280: 148–157.
27. Dejana E, Orsenigo F and Lampugnani MG. The role of adherens junctions and VE-cadherin in the control of vascular permeability. *J Cell Sci* 2008; 121(Pt 13): 2115–2122.
28. Harris ES and Nelson WJ. VE-cadherin: at the front, center, and sides of endothelial cell organization and function. *Curr Opin Cell Biol* 2010; 22: 651–658.
29. Gotsch U, Borges E, Bosse R, et al. VE-cadherin antibody accelerates neutrophil recruitment in vivo. *J Cell Sci* 1997; 110(Pt 5): 583–588.
30. Liu WY, Wang ZB, Wang Y, et al. Increasing the Permeability of the Blood-brain Barrier in Three Different Models in vivo. *CNS Neurosci Ther* 2015; 21: 568–574.
31. Gavard J and Gutkind JS. VE-cadherin and claudin-5: it takes two to tango. *Nat Cell Biol* 2008; 10: 883–88-5.
32. Sun H, Tang Y, Guan X, et al. Effects of selective hypothermia on blood-brain barrier integrity and tight junction protein expression levels after intracerebral hemorrhage in rats. *Biol Chem* 2013; 394: 1317–1324.
33. Schrade A, Sade H, Couraud PO, et al. Expression and localization of claudins-3 and -12 in transformed human brain endothelium. *Fluids Barriers CNS* 2012; 9: 6.
34. Wolburg H, Wolburg-Buchholz K, Kraus J, et al. Localization of claudin-3 in tight junctions of the blood-brain barrier is selectively lost during experimental autoimmune encephalomyelitis and human glioblastoma multiforme. *Acta Neuropathol* 2003; 105: 586–592.

35. Abbott NJ, Patabendige AA, Dolman DE, et al. Structure and function of the blood-brain barrier. *Neurobiol Dis* 2010; 37: 13–25.
36. Liu H and Kao WW. A novel protocol of whole mount electro-immunofluorescence staining. *Mol Vision* 2009; 15: 505–517.
37. Roberts WG, Whalen PM, Soderstrom E, et al. Antiangiogenic and antitumor activity of a selective PDGFR tyrosine kinase inhibitor, CP-673,451. *Cancer Res* 2005; 65: 957–966.
38. Yang P, Wu J, Miao L, et al. Platelet-derived growth factor receptor-beta regulates vascular smooth muscle cell phenotypic transformation and neuroinflammation after intracerebral hemorrhage in mice. *Crit Care Med* 2016; 44: e390–e402.
39. Yang GY, Betz AL, Chenevert TL, et al. Experimental intracerebral hemorrhage: relationship between brain edema, blood flow, and blood-brain barrier permeability in rats. *J Neurosurg* 1994; 81: 93–102.
40. Shen J, Ishii Y, Xu G, et al. PDGFR-beta as a positive regulator of tissue repair in a mouse model of focal cerebral ischemia. *J Cereb Blood Flow Metab* 2012; 32: 353–367.
41. Samuel MS, Lopez JI, McGhee EJ, et al. Actomyosin-mediated cellular tension drives increased tissue stiffness and beta-catenin activation to induce epidermal hyperplasia and tumor growth. *Cancer Cell* 2011; 19: 776–791.
42. Borkham-Kamphorst E, Alexi P, Tihaa L, et al. Platelet-derived growth factor-D modulates extracellular matrix homeostasis and remodeling through TIMP-1 induction and attenuation of MMP-2 and MMP-9 gelatinase activities. *Biochem Biophys Res Commun* 2015; 457: 307–313.
43. Usuki K, Heldin NE, Miyazono K, et al. Production of platelet-derived endothelial cell growth factor by normal and transformed human cells in culture. *Proc Natl Acad Sci U S A* 1989; 86: 7427–7431.
44. Turner PV, Pekow C, Vasbinder MA, et al. Administration of substances to laboratory animals: equipment considerations, vehicle selection, and solute preparation. *J Am Assoc Lab Animal Sci* 2011; 50: 614–627.
45. Abu-Hijleh MF, Habbal OA and Moqattash ST. The role of the diaphragm in lymphatic absorption from the peritoneal cavity. *J Anat* 1995; 186(Pt 3): 453–467.